

# 3-D Radiative Transfer Modeling of Structured Winds in Massive Hot Stars with Wind3D

A. Lobel<sup>1</sup>, J. A. Toalá<sup>2</sup>, and R. Blomme<sup>1</sup>

<sup>1</sup> Royal Observatory of Belgium, Ringlaan 3, B-1180, Brussels, Belgium

<sup>2</sup> Universidad Nacional Autónoma de México, Centro de Radioastronomía y Astrofísica, Campus Morelia, Michoacán, México

**Abstract:** We develop 3-D models of the structured winds of massive hot stars with the WIND3D radiative transfer (RT) code. We investigate the physical properties of large-scale structures observed in the wind of the B-type supergiant HD 64760 with detailed line profile fits to Discrete Absorption Components (DACs) and rotational modulations observed with IUE in Si IV  $\lambda$ 1395.

We develop parameterized input models for WIND3D with large-scale equatorial wind density- and velocity-structures, or so-called ‘Co-rotating Interaction Regions’ (CIRs) and ‘Rotational Modulation Regions’ (RMRs). The parameterized models offer important advantages for high-performance RT calculations over ab-initio hydrodynamic input models. The acceleration of the input model calculations permits us to simulate and investigate a wide variety of physical conditions in the extended winds of massive hot stars.

The new modeling method is very flexible for constraining the dynamic and geometric wind properties of RMRs in HD 64760. We compute that the modulations are produced by a regular pattern of radial density enhancements that protrude almost linearly into the equatorial wind. We find that the modulations are caused by narrow ‘spoke-like’ wind regions. We present a hydrodynamic model showing that the linearly shaped radial wind pattern can be caused by mechanical wave action at the base of the stellar wind from the blue supergiant.

## 1 Introduction

Accurate mass-loss rates of massive hot stars determined from quantitative spectroscopy are important for understanding the physical properties of the radiative wind driving mechanism that is influenced by dynamic structures on both large and small length scales in the wind. Rotational modulations and Discrete Absorption Components are important tracers of large-scale structures in the highly supersonic winds of these stars. DACs are recurring absorption features observed in UV resonance lines of many OB-stars. They drift bluewards in the absorption portion of P-Cygni profiles. DACs are caused by spiral-shaped density- and velocity structures winding up in the plane of the equator over several tens of stellar radii (e.g., Cranmer & Owocki 1996). Lobel & Blomme (2008) demonstrated with 3-D RT modeling (combined with hydrodynamic simulations) of the detailed DAC evolution in HD 64760 (B0.5 Ib) that these wind spirals are extended density waves emerging from two bright equatorial spots that rotate five times slower than the stellar surface. Detailed hydrodynamic models of its structured wind with these large density waves (or CIRs) reveal only a very small increase of less than 1 % above the smooth (symmetric) wind mass-loss rate.

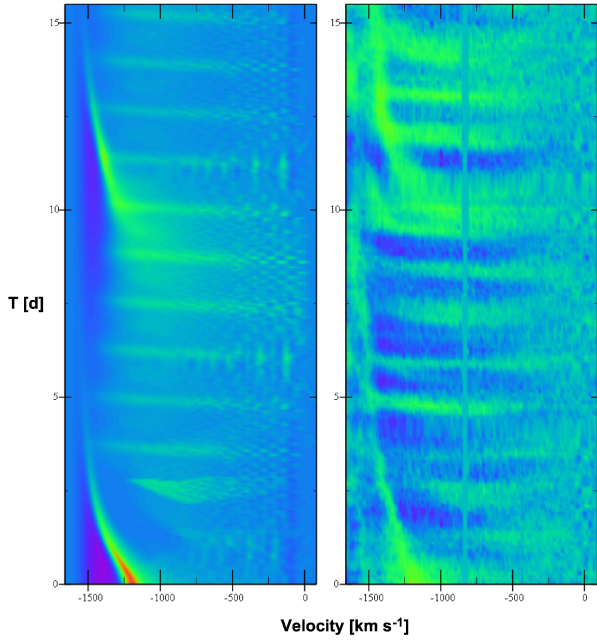


Figure 1: Dynamic spectrum of Si IV  $\lambda 1395$  observed during 15.5 d in HD 64760 (*right-hand panel*), compared to 3-D radiative transfer calculations (*left-hand panel*) with a parameterized structured wind model. Horizontal absorptions are the modulations we model in this paper.

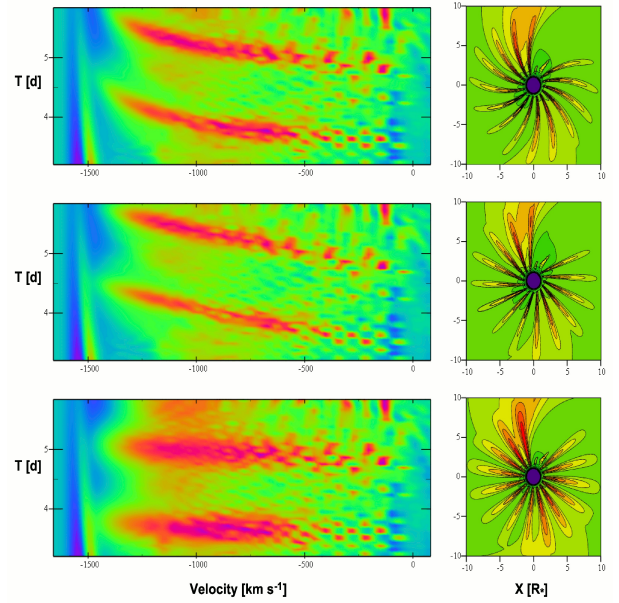


Figure 2: The curvature, incidence angle on the surface, and opening angle of the RMRs shown in the right-hand panels determine the acceleration (*upper panels*), inclination (*middle panels*), and duration (*lower panels*), respectively, of the RT calculated modulations (*left-hand panels*).

The bright surface spots produce the large-scale CIRs in the wind. The density enhancements and velocity plateaus of the CIRs yield migrating DACs with a recurrence period of 10.3 d in the UV line profiles of HD 64760. The modulations, on the other hand, show much shorter periods of  $\sim 1.2$  d and reveal a time-evolution that substantially differs from the rather slowly shifting DACs. The modulations are nearly-flat absorption features observed for only  $\sim 0.5$  d to 0.75 d with radial velocities that can range from  $\sim 0$  km s $^{-1}$  to  $\sim v_{\infty} = 1560$  km s $^{-1}$  (Massa et al. 1995; Prinja 1998). They can intersect the slowly drifting DACs and sometimes reveal a remarkable bow shape (Fullerton et al. 2006) with broad flux minima around  $\sim 930$  km s $^{-1}$ . In this paper we present a semi-empiric model of the large-scale wind structures based on detailed RT fits to the time-evolution of the modulations observed in HD 64760. We utilize the WIND3D code for performing non-LTE RT calculations (*Sect. 2*) of important diagnostic spectral lines, such as Si IV  $\lambda 1395$ . We develop *parameterized* 3-D input models for Wind3D in *Sect. 3* because they offer important advantages for high-performance RT calculations over ab-initio hydrodynamic input models. The acceleration of the input model calculations permits us to model and investigate a much broader range of 3-D physical conditions in the wind.

## 2 Parametrization of Wind3D Input Models

Wind3D computes the 3-D non-LTE transport of radiation for the 2-level atom in optically thick resonance lines formed in scattering-dominated extended stellar winds. It lambda-iterates the line source function on a Cartesian grid of  $71^3$  points. The radiative transfer equation is solved in parallel over a mesh of  $701^3$  voxels using the converged line source function. Typical computation times with WIND3D are  $\sim 5$  h for iterating the line source function, and  $\sim 12$  h for calculating the dynamic line profile variability at 90 viewing angles using 16 CPUs.

We develop a new software module in WIND3D for semi-empiric modeling of large-scale equatorial wind density- and velocity-structures. The computer code integrates the time-independent momentum balance equation of radiation-driven rotating winds following Castor, Abbott & Klein (CAK, 1975). First, we parametrize the large-scale density structures in a stationary model of the equatorial wind with:

$$\rho(x, y, \psi) = \rho_0(r) \left( 1 + A(r) \sin^m \left( \psi n + 2\pi n f_c \left( \frac{R_\star - \sqrt{(x - x_0)^2 + y^2}}{R_\star - R_{\text{mod}}} \right) \right) \right), \quad (1)$$

where  $r^2=x^2+y^2$ ,  $R_{\text{cr}} \leq r \leq R_{\text{mod}}$ ,  $-\pi \leq \psi \leq \pi$ , and  $R_{\text{mod}}$  is the outer radius of the wind model.  $x_0=R_\star \sin(\psi_0)$ , where  $\psi_0$  is the incidence angle of the equatorial wind structures on the stellar surface, and  $0 \leq \psi_0 \leq \pi/2$ .  $\rho_0(r)$  is the density of the smooth (unperturbed) equatorial wind.  $n$  denotes the number of large-scale wind structures with enhanced density in one hemisphere, and  $m$  is an even exponent of the sine function that sets the opening angle or the tangential width of the wind structures. In wind regions where the sine function vanishes the local wind density equals the smooth wind density. The term in Eq. (1) with  $f_c$ , where  $0 \leq f_c \leq 1$ , determines the curvature of the wind structures between  $R_\star$  and  $R_{\text{mod}}$ . If  $f_c=1$ , they turn completely around the star over  $2\pi$  from the surface radius  $R_\star$  to  $R_{\text{mod}}$ . In case  $f_c=0$ , the structures do not curve at all and stay strictly radial (linear) in the wind, ordered in equal sectors around the star. We parametrize the density contrast of the large-scale wind structures with the function  $A$  in Eq. (1):

$$A(r) = c_1 \exp \left( - \left( \frac{r}{R_\star} - c_2 \right)^2 + c_3 \left( \frac{r}{R_\star} \right)^2 + c_4 \right), \quad (2)$$

where  $c_{1,2,3,4}$  are constants. They determine the detailed density profile compared to  $\rho_0(r)$ . We vary the four constants until the parameterized density profile best fits the density contrast of the CIRs in the hydrodynamic wind model of HD 64760.

Next, with the parameterized radial wind density-structure we compute the corresponding radial wind velocity-structure for the  $\alpha$  parameter of CAK theory set equal to 1/2 in hot stars with  $20 \text{ kK} \leq T_{\text{eff}} \leq 30 \text{ kK}$ . We solve the CAK momentum balance equation in 1-D for many angles  $\psi$ , and include the centrifugal force in the equatorial plane due to the photospheric rotation velocity  $v_{\text{rot}}$ . With the conservation of angular momentum the equatorial tangential wind velocity is  $v_{\text{rot}} R_\star / r$ , which becomes negligibly small in the highly supersonic outer regions of the parameterized wind models. We integrate the momentum equation together with the mass continuity equation towards the surface from a typical outer (reference) radius  $r_{\text{ref}} \geq 30 R_\star$  with the boundary condition  $v(r = r_{\text{ref}}) = v_\infty$ , down to the critical point  $R_{\text{cr}}$  of the wind. The value of the mass-loss rate for calculating the CAK line force is computed with Eq. (5) of Lobel & Blomme (2008), but which typically increases the structured wind mass-loss rate by less than  $\sim 1\%$  in the best-fit 2-spot model. We find that the radial wind velocity-structure computed with the CAK wind-momentum equation integration method, using parameterized stationary wind density models, compares very closely to the hydrodynamic wind velocity model of HD 64760 (Lobel & Toalá 2009).

### 3 Radiative Transfer Modeling of Rotational Modulations

Figure 1 compares the dynamic spectrum of Si IV observed over 15.5 d in HD 64760 (*right-hand panel*) and computed with WIND3D (*left-hand panel*) using a parameterized structured wind model. The slowly bluewards migrating upper and lower DACs result from two spiral-shaped CIRs shown in the right-hand panels of Fig. 2. The nearly horizontal absorption in the modulations is due to

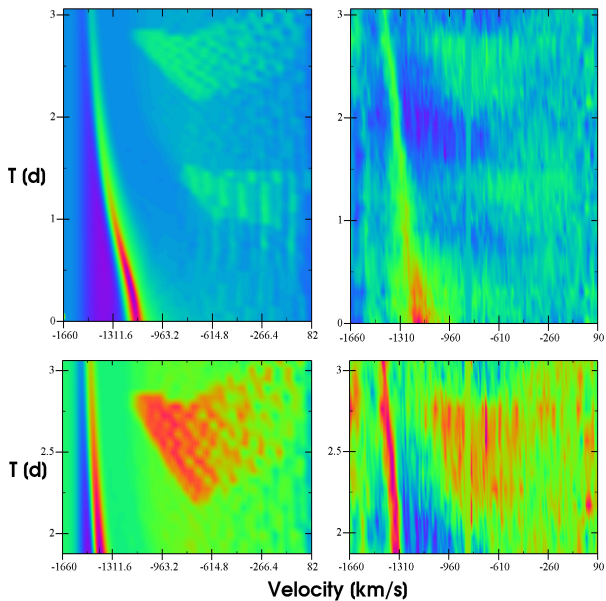


Figure 3: The upper panels show two modulations computed with Wind3D (*left-hand panel*) and observed over  $\sim 3.1$  d (*right-hand panel*) in Si IV  $\lambda 1395$  of HD 64760. The lower panels show the best fit (*left*) and the observed (*right*) upper ‘bow shaped’ modulation in more detail (*see text*).

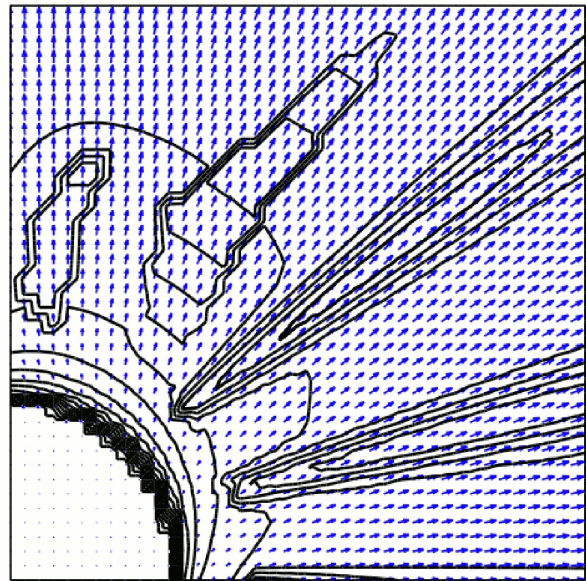


Figure 4: Parameterized model of the equatorial wind-density structure of HD 64760 computed with 3-D RT fits to the modulations in Fig. 3. The solid drawn lines show density contours of the modulations. The blue arrows mark the local wind velocity to  $\sim 3 R_{\star}$  above the stellar surface.

almost linearly shaped density enhancements and local wind velocity variations that radially protrude into the equatorial wind. The RMRs have maximum tangential widths of less than  $\sim 1 R_{\star}$  across the wind. Our parameterized RT modeling reveals that the RMRs are *linear* density enhancements through the wind because the modulations of HD 64760 stay flat beyond  $1000 \text{ km s}^{-1}$ . The upper panels of Fig. 2 show that the (radial velocity) acceleration of the modulations is too slow (*left-hand panel*) in case the RMRs curve too quickly over  $\sim 10 R_{\star}$  above the stellar surface (*right-hand panel*). Hence, the RMRs are large-scale density- and velocity-structures in the supersonically (radiatively) accelerating equatorial wind. The parameterized best-fit modeling method shows that the RMRs are centered around the star with small inclination angles of  $\leq 6^{\circ}$  from the radial direction (the rather narrow RMRs have small incidence angles on the stellar surface in the middle panel of Fig. 2). We also compute opening angles of  $\leq 10^{\circ}$  for the RMRs at the wind base to correctly fit the observed duration of the modulations.

Figure 3 shows a portion of the dynamic spectrum in Fig. 1 observed between 0 d and 3.1 d (*upper right-hand panel*). The lower DAC in Fig. 3 slowly shifts bluewards from  $\sim 1100 \text{ km s}^{-1}$  to  $\sim 1400 \text{ km s}^{-1}$ , while two modulations are observed around 1.2 d (*lower modulation*) and 2.5 d (*upper modulation*). The upper modulation is observed during  $\sim 0.7$  d and reveals a somewhat curved shape, whereas the lower one occurs during  $\sim 0.5$  d showing a more irregular absorption pattern below  $\sim 800 \text{ km s}^{-1}$ . We delineate the borders of the wind density enhancements in two RMRs above the stellar surface and compute the radial wind velocity structure of the parameterized model by integrating the CAK momentum equation (*Sect. 2*). The lower panels of Fig. 3 show the observed (*right-hand panel*) and best-fit (*left-hand panel*) dynamic flux profile of the upper modulation computed with WIND3D. We fit the peculiar wedge-like shape at its short-wavelength side in detail by decreasing the opening angle of the density enhancement borders of the RMR beyond  $1 R_{\star}$  above the

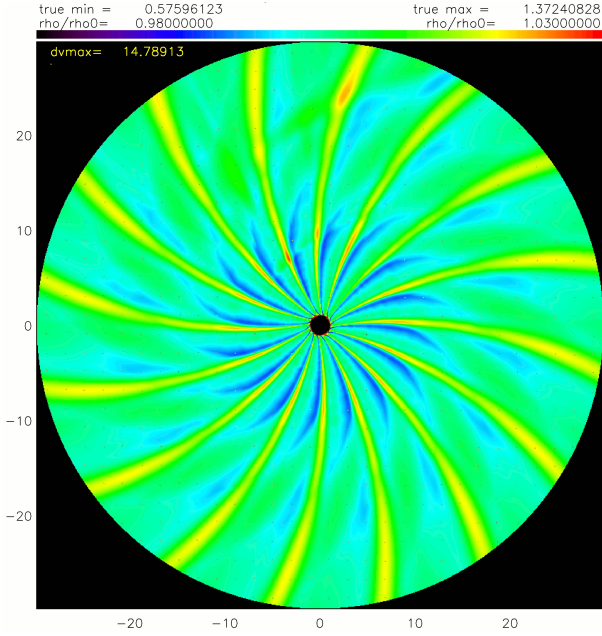


Figure 5: Yellow colors mark density enhancements in the hydrodynamic wind model for rotational modulations of HD 64760 (*see text*).

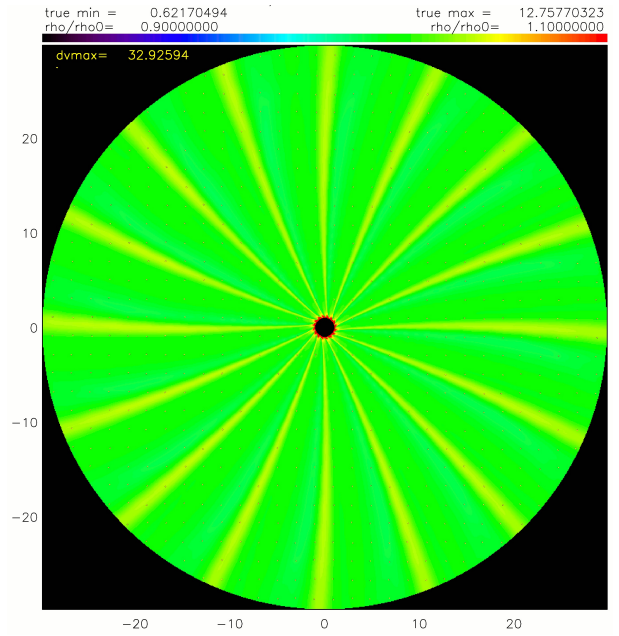


Figure 6: The RMRs in the hydro model are less curved for a horizontal wave at the wind base that rotates 5 times slower than the star.

stellar surface, shown in Fig. 4. The radial wind velocity-structure of the upper modulation does not exceed  $\sim 1200 \text{ km s}^{-1}$  around 2.8 d, and it does not intersect the velocity of the lower DAC around  $\sim 1400 \text{ km s}^{-1}$ . The wind density and velocity model of the upper modulation in Fig. 4 does therefore not exceed a distance of  $\sim 2.5 R_*$  above the stellar surface because the smooth-wind velocity exceeds  $\sim 1200 \text{ km s}^{-1}$  only beyond that radius. We therefore attribute the remarkable bow shape (called ‘phase-bowing’) observed in the upper modulation to the intrinsically curved shape of the front and backside borders of the RMR we model in detail in Fig. 4. Several modulations observed between 5.5 d and 9 d in Fig. 1 do not show a clear bow shape (they are in fact strictly flat), although their flux profiles compare closely to the modulations that show the bow shape in Fig. 3. The remarkable bow shape is rather peculiar and results from the slightly curved shapes of a number of RMRs in the model. Modulations without the bow shape are due to RMRs that protrude strictly radially into the wind. Best fits to the detailed flux profiles in the modulations show that the maximum density of the RMRs does not exceed the smooth-wind density by  $\sim 17 \%$ , or about half the maximum density contrast of  $\sim 31 \%$  in the CIR model of the lower DAC. Hence, the RMRs do not appreciably increase the wind mass-loss rate of HD 64760, also concluded for the CIR models in Lobel & Blomme (2008).

Owocki, Cranmer, & Fullerton (1995) presented a kinematic model for the spiral density wind features that satisfies the time-dependent mass-continuity relation. We further investigate the results of the (time-independent) semi-empiric modeling method with time-dependent hydrodynamic models. We compute hydrodynamic test models of RMRs in HD 64760 with ZEUD3D. We introduce a propagating pressure wave at the lower wind boundary near the stellar surface. The wave propagates horizontally over the stellar equator. It periodically alters the radiative wind acceleration due to mechanical momentum imparted upwards to the wind by wave action. Figure 5 shows the density contrast computed in the wind out to  $30 R_*$  for a wave with a radial velocity amplitude of  $v_{\text{sound}}/100$  at the stellar surface. The wavelength is set to 1/16 of the stellar circumference and it co-rotates counter-clockwise with the surface ( $\omega_{\text{wave}} = \omega_{\text{star}}$ ). The density structure at the wind base is very intricate and converges into 16 rather narrow and stable density enhancements extending almost radially through the wind. The tangential width of the wind density enhancements (*in yellow color*) is  $\leq 1 R_*$ ,

comparable to the parameterized model we find for the RMRs. The hydrodynamic model in Fig. 6 shows a decrease of the intrinsic curvature of these narrow wind features for a wave that rotates 5 times slower than the surface ( $\omega_{\text{wave}} = \omega_{\text{star}} / 5$ ). The velocity amplitude of the wave is increased to  $2 \times v_{\text{sound}}$ , producing somewhat larger densities of  $\sim 8\%$  above the smooth-wind density. The near-linear regular pattern in the hydrodynamic wind model is almost identical to the spoke-like RMRs we compute with parameterized models of the modulations in HD 64760. The maximum density contrast of the hydrodynamic wind pattern is however too small compared to  $\sim 17\%$  of the RMRs to fit the flux profiles observed in the modulations. Further hydrodynamic modeling is required to simulate the conditions of the best-fit parameterized wind model in more detail, and to investigate the formation physics of the large-scale wind pattern that causes the modulations observed in HD 64760.

## 4 Conclusions

We perform 3-D RT calculations with WIND3D of the rotational modulations observed in Si IV  $\lambda 1395$  of HD 64760. We find that the horizontal absorptions in the line are caused by a very regular pattern of almost linearly shaped radial density- and velocity-variations in the equatorial wind out to  $\sim 10 R_{\star}$  above the stellar surface. The density in the RMRs does not exceed  $\sim 17\%$  of the smooth-wind density, and hence they do not appreciably increase the stellar mass-loss rate. Hydrodynamic models computed with ZEUS3D show that RMRs can result from mechanical wave action at the base of the stellar wind producing the rather narrow ‘spoke-like’ wind regions in a regular geometric pattern centered around the star. We conjecture that the waves are caused by non-radial pulsations (for example discussed in Kaufer et al. 2006) of HD 64760.

## References

- Castor, J. I., Abbott, D. C. & Klein, R. I. 1975, ApJ, 195, 157  
Cranmer, S. R., & Owocki, S. P. 1996, ApJ, 462, 469  
Fullerton, A. W., Massa, D. L., Prinja, R. K., Owocki, S. P., & Cranmer, S. R. 1997, A&A, 327, 699  
Kaufer, A., Stahl, O., Prinja, R. K., & Witherick, D. 2006, A&A, 447, 325  
Lobel, A., & Blomme, R. 2008, ApJ, 678, 408  
Lobel, A., & Toalá, J. A. 2009, in *Eta Carinae in the Context of the Most Massive Stars*, Proc. of XXVIIth IAU GA, Highlights of Astronomy 14, ed. I. F. Corbett, p. 20, arXiv:0910.3158v1  
Massa, D., et al. 1995, ApJ, 452, L53  
Owocki, S. P., Cranmer, S. R., & Fullerton, A. W. 1995, ApJ 453, L37  
Prinja, R. K. 1998, in *Cyclical Variability in Stellar Winds*, eds. L. Kaper & A. W. Fullerton, 92, Springer-Verlag, Heidelberg